2974–2983 *Nucleic Acids Research, 2009, Vol. 37, No. 9* *Published online 18 March 2009*
doi:10.1093/nar/gkp173

The RRM domain in GW182 proteins contributes to miRNA-mediated gene silencing

Ana Eulalio, Felix Tritschler, Regina Büttner, Oliver Weichenrieder, Elisa Izaurralde* and Vincent Truffault

Max Planck Institute for Developmental Biology, Spemannstrasse 35, D-72076 Tübingen, Germany

Received 8 February 2009; Revised 2 March 2009; Accepted 3 March 2009

ABSTRACT

Proteins of the GW182 family interact with Argonaute proteins and are required for miRNA-mediated gene silencing. These proteins contain two structural domains, an ubiquitin-associated (UBA) domain and an RNA recognition motif (RRM), embedded in regions predicted to be unstructured. The structure of the RRM of *Drosophila melanogaster* GW182 reveals that this domain adopts an RRM fold, with an additional C-terminal α-helix. The helix lies on the β-sheet surface, generally used by these domains to bind RNA. This, together with the absence of aromatic residues in the conserved RNP1 and RNP2 motifs, and the lack of general affinity for RNA, suggests that the GW182 RRM does not bind RNA. The domain may rather engage in protein interactions through an unusual hydrophobic cleft exposed on the opposite face of the β-sheet. We further show that the GW182 RRM is dispensable for P-body localization and for interaction of GW182 with Argonaute-1 and miRNAs. Nevertheless, its deletion impairs the silencing activity of GW182 in a miRNA target-specific manner, indicating that this domain contributes to silencing. The conservation of structural and surface residues suggests that the RRM domain adopts a similar fold with a related function in insect and vertebrate GW182 family members.

INTRODUCTION

Proteins of the GW182 family are essential components of mRNA processing bodies or P-bodies (1–3). They interact with the Argonaute proteins and are required for miRNA-mediated gene silencing in animal cells (3–5). GW182 proteins are characterized by the presence of two to three distinctive blocks of glycine–tryptophan repeats (referred to as N-terminal, middle and C-terminal GW-repeats) and two predicted structured domains: a central ubiquitin-associated (UBA) domain, and a C-terminal RNA recognition motif (RRM). Furthermore, a predicted unstructured, glutamine-rich (Q-rich) region lies between the UBA and the RRM domains [Figure 1A; (1, 6)].

The role of GW182 proteins in the miRNA pathway is well established in *Drosophila melanogaster* cells. Here, depleting the sole GW182 family member found in insects suppresses silencing of miRNA targets, irrespective of whether they are translationally repressed or directed to degradation (5–9). In these cells depleted of GW182 there is no decrease in the expression levels of AGO1 [the Argonaute protein dedicated to the miRNA pathway in *D. melanogaster*, (9)], suggesting that Argonaute proteins cannot silence miRNA targets in the absence of GW182. These and additional observations lead us to propose that target silencing by miRNAs is effected by a protein complex consisting minimally of an Argonaute and a GW182 protein (5,9).

In other organisms, demonstrating that GW182 proteins play a role in silencing has been hampered by the existence of multiple paralogs, with partially redundant functions. For example, vertebrate genomes encode three GW182 paralogs: TNRC6A/GW182, TNRC6B and TNRC6C (4,6); and the human proteins were shown to associate with all four Argonaute proteins (AGO1–4) and with a common set of miRNA targets (10–13). Moreover, in human cells depleting TNRC6A or B partially relieves silencing of siRNA and miRNA targets (10–14).

The *Caenorhabditis elegans* genome encodes two divergent members of the GW182 protein family (AIN-1 and AIN-2); these proteins contain motifs similar to the N-terminal GW-repeats of vertebrate and insect proteins, but lack the Q-rich region, the UBA and the RRM domains (4,6,15–17). Both proteins interact with *C. elegans* Argonaute proteins 1 and 2 [ALG-1, ALG-2; (15,16)]. Moreover, co-depleting AIN-1 and AIN-2 suppresses silencing more efficiently than depleting each protein individually, indicating that the role of these proteins in the miRNA pathway is also partially redundant (16,17).

The N-terminus of all members of the GW182 family, characterized by several GW-repeats, mediates the

*To whom correspondence should be addressed. Tel: +49 7071 601 1350; Fax: +49 7071 601 1353; Email: elisa.izaurralde@tuebingen.mpg.de

interaction with Argonaute proteins (6,18). How the other domains of GW182 proteins affect silencing activity is less well understood. For *D. melanogaster* GW182, we have shown that the N-terminal region containing GW repeats, together with the UBA domain and the Q-rich region is necessary and sufficient to localize GW182 to P-bodies (6). Furthermore, this protein fragment promotes the accumulation of AGO1 in P-bodies, a process that depends on the interaction with GW182 in *D. melanogaster* cells (6).

In *C. elegans*, AIN-1 and AIN-2 interact with the Argonaute proteins and function in the miRNA pathway, yet these proteins lack a UBA domain, the Q-rich region and the RRM domain. This raises the question: how do these domains affect the activity of vertebrate TNRC6A–C and insect GW182?

In this study, we characterized the RRM domain of *D. melanogaster* GW182. We show that this domain adopts an RRM fold in solution, with an additional C-terminal α-helix shielding the β-sheet surface, which in canonical RRMs is involved in RNA binding. This, together with the lack of general affinity for RNA and the absence of aromatic residues in the conserved RNP1 and RNP2 motifs, suggests that the GW182 RRM is not involved in RNA recognition. Rather, this domain may engage in protein–protein interactions through an unusual hydrophobic cleft exposed on its helical side. We also show that the RRM domain is not required for GW182 to interact with AGO1 or with miRNAs. Furthermore this domain is dispensable for the accumulation of both GW182 and AGO1 in P-bodies. Unexpectedly, however, the GW182 RRM contributes to silencing of a subset of miRNA targets.

MATERIALS AND METHODS

Cloning, expression and purification of the RRM domain of *D. melanogaster* GW182

The sequence encoding the RRM domain of *D. melanogaster* GW182 (gi:18447359; Trp1114 to His1198) was cloned into the pETM60 vector (derived from pET24-d; Novagen). The protein was expressed in the *Escherichia coli* strain BL21(DE3) Rosetta II at 20°C overnight. To uniformly label GW182 RRM with $^{15}N/^{13}C$ or ^{15}N, cells were grown in M9 minimal medium supplemented with $^{15}NH_4Cl$ with or without $^{13}C_6$-glucose. The protein was purified by affinity chromatography using Ni-NTA (Ni-nitrilotriacetic acid) HiTrap chelating HP columns (GE Healthcare). The tag was then cleaved by overnight exposure to TEV protease. The protein was purified to homogeneity by two subsequent gel filtrations using a HiLoad 26/60 Superdex 75 preparative-grade column (GE Healthcare). The purity of the resulting protein, consisting of the cloned sequence plus an additional four residues at the N-terminus, was confirmed by sodium dodecyl sulfate-polyacrylamide gel electrophoresis. Samples for nuclear magnetic resonance (NMR) spectroscopy were prepared at 1 mM in PBS (pH 7) containing 1 mM dithiothreitol.

NMR measurement and structure calculation

All spectra were recorded at 298 K on Bruker AVIII-600 and AVIII-800 spectrometers. Backbone sequential assignments were completed using standard triple resonance experiments, implemented using selective proton flipback techniques for fast pulsing (19). Aliphatic side-chain assignments were completed by a combination of CCH-COSY and CCH-TOCSY experiments, while aromatic assignments were made by linking aromatic spin systems to the respective $C^{\beta}H_2$ protons, in a 2D-NOESY spectrum. Stereospecific assignments and the resulting $\chi 1$ rotamer assignments were determined for 34 of 57 prochiral $C^{\beta}H_2$ protons and for the $C^{\gamma}H_3$ groups of all three valine residues. Assignments of $\chi 1$ rotamers were also available for all four isoleucine residues and six of seven threonine residues. Assignment of $\chi 2$ rotamers were made for all 4 isoleucine and 8 of 11 leucine residues.

Distance data were derived from a set of five 3D-NOESY spectra, including the heteronuclear edited NNH-, CCH- and CNH-NOESY spectra (20) in addition to conventional ^{15}N- and ^{13}C-HSQC-NOESY spectra, and a 2D-NOESY spectrum recorded on an unlabeled sample. Distance and dihedral angle restraints applied for the 82 high-confidence predictions found by the program TALOS (21) and 38 hydrogen bond restraints were derived as detailed elsewhere (22).

Refinement was carried out by comparing all five of the experiments and back-calculated 3D-NOESY-HSQC and 3D-HSQC-NOESY-HSQC spectra (in house software). This process adjusted side-chain rotamers for several residues.

Structures were calculated with XPLOR (NIH version 2.9.4) using standard protocols with modifications as described (23). For the final set, 50 structures were calculated and 23 chosen on the basis of lowest restraint violations. An average structure was calculated and regularized to give a structure representative of the ensemble.

DNA constructs and transfection of S2 cells

Luciferase reporters and plasmids for expression of miRNAs and of λN-HA protein fusions were described before (6,7,24). GW182-ΔRRM was generated by site-directed mutagenesis using the plasmid pAc5.1B-λN-HA-GW182 as template, and the Quick Change mutagenesis kit from Stratagene.

Transfections of S2 cells were performed in 6-well plates, using Effectene transfection reagent (Qiagen). The transfection mixtures contained 0.1 μg of firefly luciferase (F-Luc) reporter plasmid, 0.4 μg of the *Renilla* transfection control and 0.5 μg of plasmids expressing miRNA primary transcripts or the corresponding vector without insert. When indicated, 0.025 μg of plasmids expressing recombinant proteins were cotransfected as indicated in the figure legends.

Firefly and *Renilla* luciferase activities were measured 3 days after transfection using the Dual-Luciferase Reporter Assay System (Promega). Total RNA was isolated using TriFast (Peqlab Biotechnologies).

RNA interference, northern and western blotting

RNA interference, northern and western blotting were performed as described before (6,7). Anti-AGO1 antibodies were purchased from Abcam (catalog number ab5070; dilution 1:1000). Bound primary antibodies were detected with alkaline-phosphatase-coupled secondary antibodies (Western-Star kit from Tropix). HA-tagged proteins were detected using anti-HA-Peroxidase [High Affinity (3F10) Roche, catalog number 12013819001] at a 1:5000 dilution. The interaction between GW182 and endogenous AGO1 or miRNAs was tested as described (9).

Immunofluorescence

Three days after transfection, S2 cells were allowed 15 min to adhere to Poly-D-Lysine-coated coverslips, washed once in serum-free medium and fixed with 4% paraformaldehyde in PBS for 15 min, followed by 5 min incubation in methanol at −20°C. After fixing, cells were washed in PBS, permeabilized for 5 min with PBS containing 0.5% Triton X-100 and washed again with PBS. Cells were stained with affinity-purified anti-Tral antibodies (25) diluted 1:250 in PBS containing 1% BSA. Alexa-594-coupled goat anti-rat secondary antibody (Molecular probes, catalog number A11007) was used at a dilution of 1:1000. HA-tagged proteins were detected with a monoclonal anti-HA antibody (Covance Research Products, catalog number MMS-101P) diluted 1:1000 in PBS containing 1% BSA. Alexa Fluor 594-coupled or Alexa Fluor 488-coupled goat anti-mouse secondary antibody (Molecular probes, catalog numbers A11001 and A11005, respectively) was used at a dilution of 1:1000. Cells were mounted using Fluoromount-G (Southern Biotechnology Associates, Inc.). Images were acquired using a Leica TCS SP2 confocal microscope.

Data Bank accession numbers

The chemical shifts and coordinates of the structure have been deposited in the BioMagResBank (accession code 16206) and PDB (accession code 2WBR).

RESULTS

Solution structure of the RRM domain of *D. melanogaster* GW182

The RRM domain of *D. melanogaster* GW182 (GW182 RRM, residues S1116 to H1198) adopts an RRM fold in solution comprising the typical $\beta_1\alpha_1\beta_2\beta_3\alpha_2\beta_4$ topology, where a four-stranded antiparallel β-sheet is flanked on one side by two α-helices [α1 and α2; Figure 1B; (26,27)]. The domain also contains a third, C-terminal α-helix (α3), which covers the face of the β-sheet that in canonical RRMs is involved in RNA-binding (Figure 1B). A similar C-terminal α-helix lies in the same location in a number of other RRM domains [reviewed in (27)]; of those, the N-terminal RRM domain of U1A [Figure 1C; (26,28,29)], the RRM3 domain of $U2AF^{65}$ [Figure 1D; (30)] and the quasi RRM1 domain of hnRNP F [Figure 1E; (31)] are well characterized and superpose with root mean square deviation (r.m.s.d.) values of 2.28, 2.38 and 2.42 Å, respectively (for alignable residues). GW182 RRM also contains a short β-strand (β3′) in loop L5, which forms a small β-hairpin (β-turn of type II) with the N-terminal portion of β-strand β4 (Figure 1B).

The ensemble of 23 lowest energy NMR structures (Supplementary Data 1) has a good r.m.s.d. (calculated over 80 structured residues) of 0.39 Å for backbone atoms and of 0.83 Å for all non-hydrogen atoms (Table 1). The restraint violations are also very low, with the final set having, on an average, three violations of distance restraints >0.09 Å per structure and one dihedral restraint violation >1 Å.

GW182 RRM lacks RNA binding properties

Canonical RRM domains are characterized by two conserved sequence signatures: RNP1 ([RK]-[G]-[**FY**]-[GA]-[**FY**]-[ILV]-[X]-[FY]), located on β-strand β3, and RNP2 ([ILV]-[**FY**]-[ILV]-X-N-L) located on β-strand β1 [Figure 2A; reviewed in (27)]. These strands provide aromatic side chains to the surface of the β-sheet (positions 3, 5 in RNP1 and position 2 in RNP2, bold characters). In GW182 RRM, the RNP1 (QG**IA**L**C**KY) and RNP2 (L**LL**KNL) motifs deviate from the consensus signature in that the aromatic residues that usually play a key role in nucleic acid binding (27) are replaced by aliphatic residues (L1120 in β1, I1154 and L1156 in β3; Figure 2A and B). Furthermore, these residues together with W1118 (in β1) contribute to hydrophobic interactions with the C-terminal α-helix (residues V1192 and I1195 in α3; Figure 2B, red dots). The C-terminal α-helix is further stabilized by a hydrogen bond between the side chains of H1198 in α3 and Y1149 in β2 (Figure 2B). All of these residues are either conserved or conservatively substituted in vertebrate TNRC6A–C proteins (Figure 2A), indicating that in GW182 RRMs the interaction of helix-3 with the β-sheet surface is a conserved feature (Figure 2A and B).

Given these tight aliphatic methyl–methyl contacts (349 $Å^2$ total buried surface), we consider it unlikely that helix α3 would move away from the observed position, like it does when the U1A RRM domain binds RNA [Figure 1C; (28,29)]. Even if it did, the exposed β-sheet surface would be hydrophobic and would not expose any classical RNA-binding features (Figure 2B).

GW182 RRM is therefore similar to the quasi RRM domains (qRRM1 and qRRM2) of hnRNP F, where the α3 helix is equally unlikely to liberate the β-sheet surface [Figure 1E; (31)]. Nevertheless, the qRRM1 domain of hnRNP F binds RNA. This RNA binding occurs at an alternative surface of the domain that is positively charged and includes the equivalent of the β3′/β4 hairpin loop as well as loops L1 and L3 (Figure 1E). Mutagenesis and NMR-shift perturbation experiments revealed both basic and aromatic side chains are involved in RNA binding [Figure 2A, magenta residues: R16 (β1), W20 (L1), R52 (L3), R75-H80-R81 and Y82 (hairpin β3′- β4), and F86 (β4); (31)]. In the GW182 RRM none of these residues is conserved (Figure 2A). Furthermore, the GW182 RRM

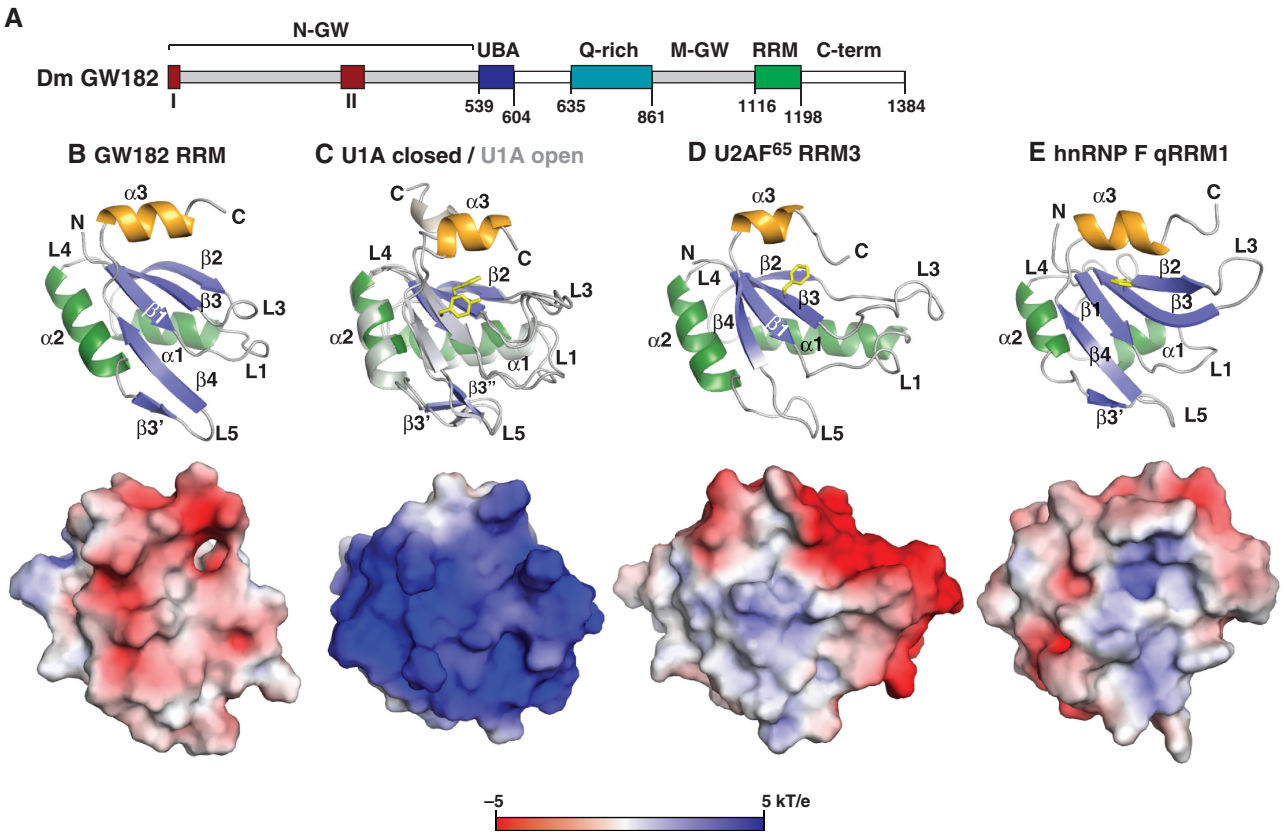

Figure 1. Solution structure of the RRM domain of *D. melanogaster* GW182. (**A**) Domain organization of GW182. N-GW and M-GW: N-terminal and middle GW repeat-containing regions, respectively; Q-rich: region rich in glutamine. C-term: C-terminal region. Red boxes I and II: two conserved motifs within the N-terminal GW repeats. Amino acid positions at domain boundaries are indicated. (**B**) Solution structure of *D. melanogaster* GW182 RRM. (**C**) Solution structure of U1A RRM in the closed conformation (closed; PDB-ID: 1FHT) superimposed on the crystal structure of human U1A RRM in the open conformation (open; in gray; PDB-ID: 1URN) with the β-sheet exposed as observed upon RNA binding. (**D**) Solution structure of human U2AF^{65} RRM3 [(30); PDB-ID: 1O0P]. (**E**) Solution structure of human hnRNP F qRRM1 [(31); PDB-ID: 2HGL]. Top panels: ribbon representation showing the β-sheet surface normally involved in RNA binding. β-strands are colored in blue and α-helixes are colored in green as in reference (30). The C-terminal α-helix is colored in orange. Side chains of conserved aromatic residues in RNP1 and RNP2 motifs are shown as yellow sticks. Lower panels: corresponding surface representations colored according to the electrostatic surface potential (blue and red colors indicate positive and negative potential, respectively, ramped from −5 kT/e to +5 kT/e using the Adaptive Poisson Boltzmann Server tool (32). All structure representations were done in PyMol (http://www.pymol.org).

lacks any positively charged surface patch that would be indicative of RNA binding (Figure 1B versus 1E, lower panels), arguing against an hnRNP F-like mode of RNA recognition.

In agreement with the assumption that GW182 RRM is unlikely to bind RNA either in a canonical or in the quasi-canonical mode, no detectable RNA-binding activity was observed *in vitro*. Indeed, the GW182 RRM did not detectably interact with an oligomeric RNA consisting of 15 or 30 uracyls (poly(rU)$_{15,30}$, as shown by analytical size exclusion chromatography measurements (data not shown). We also tested RNA binding by NMR, which detects low-affinity interactions (34); however, no binding (i.e. chemical shift changes) was detected, even when up to an equimolar amount of poly(rU)$_{15}$ or poly(rU)$_{30}$ was added to purified GW182 RRM (Supplementary Data 2). Although the possibility that GW182 RRM binds a specific RNA sequence motif cannot be ruled out, the lack of general affinity for RNA together with the absence of critical RNA-binding residues suggest that this domain does not bind RNA.

GW182 RRM may interact with other proteins via an unusual hydrophobic cleft

Several studies showed that some RRMs mediate protein–protein interactions, in addition to or instead of recognizing RNA [reviewed in (27)]. This is the case, for instance, for the RRM domains of the exon-junction complex protein Y14 (35), the nonsense-mediated mRNA decay effector UPF3 (36) and the C-terminal RRM (RRM3) of human U2AF^{65}, which also bears a C-terminal α-helix (α3) across its β-sheet surface [Figure 1D; (30)].

While Y14 and UPF3 bind their protein partners via the β-sheet surface generally used by RRMs to bind RNA (35,36), the RRM3 of U2AF^{65} recruits the N-terminal peptide of Splicing Factor 1 (SF1) via its α-helical surface. The C-terminal end of the SF1 peptide inserts into a hydrophobic pocket between α-helices α1 and α2 and the adjacent loops L1 and L5 [Figure 3C; (30)].

Interestingly, GW182 RRM has an even larger hydrophobic cleft between the α-helices and adjacent

Table 1. Structural statistics and atomic r.m.s.d.[a]

Structural statistics	SA		<SA>$_r$	
r.m.s.d. from distance restraints (Å)[b]				
All (417)	0.020 ± 0.001		0.021	
Intra-residue (72)	0.025 ± 0.001		0.024	
Inter-residue sequential (139)	0.012 ± 0.001		0.012	
Medium range (69)	0.034 ± 0.003		0.037	
Long range (137)	0.021 ± 0.001		0.022	
H-bond (37)	0.011 ± 0.001		0.011	
r.m.s.d. from dihedral restraints (226)	0.23 ± 0.01		0.23	
H-bond restraints average (Å/deg)[c] (37)	2.17 ± 0.12/13.7 ± 7.2		2.17 ± 0.12/13.6 ± 7.2	
H-bond restraints min–max (Å/deg)[c]	1.94–2.50/3.71–46.32		1.94–2.52/4.04–46.5	
Deviations from ideal covalent geometry				
Bonds (Å × 10^{-3})	6.83 ± 0.001		6.77	
Angles (deg)	0.636 ± 0.004		0.632	
Impropers (deg)	2.12 ± 0.05		2.19	
Structure quality indicators[d]				
Ramachandran map regions (%)	94.9/5.1/0.0/0.0		94.9/5.1/0.0/0.0	
Atomic r.m.s. differences (Å)[e]	SA versus <SA>		SA versus <SA>$_r$	
	Backbone	All	Backbone	All
Secondary structure[f]	0.39 ± 0.07	0.83 ± 0.08	0.53 ± 0.13	1.03 ± 0.14
<SA> versus <SA>$_r$[g]	0.37	0.69		

[a]Structures are labeled as follows: SA, the set of 23 final simulated annealing structures; <SA>, the mean structure calculated by averaging the coordinates of SA structures after fitting over secondary structure elements; <SA>$_r$, the structure obtained by regularizing the mean structure under experimental restraints.
[b]Numbers in brackets indicate the number of restraints of each type.
[c]Hydrogen bonds were restrained by treating them as pseudo-covalent bonds (see Materials and Methods section). The average and minimum/maximum for distances and acceptor antecedent angles are stated for restrained hydrogen bonds.
[d]Determined using the program PROCHECK (33). Percentages are for residues in allowed/additionally allowed/generously allowed/disallowed regions of the Ramachandran map.
[e]Based on heavy atoms superimpositions.
[f]Defined as residues W1118-H1198.
[g]The r.m.s. difference for superimposition over ordered residues.

loops, which is rather unique among RRM domains (Figure 3A–D). Compared with U2AF^{65} RRM3 the space is liberated primarily by the orientation of the β3′/β4 hairpin (loop L5) such that side chains do not reach to contact residues on the opposing α-helix α1 (Figure 3A). The entire cleft is lined by aliphatic side chains [Figure 2A, residues in red: L1121 (β1), L1133 and L1136 (α1), L1172 (α2), L1177 (β3′) and I1182 (β4)], creating a hydrophobic patch of considerable size, which is usually not exposed to the solvent (Figure 3A). Each of these residues is conserved in vertebrate TNRC6s (Figure 2A). It is therefore likely that this large hydrophobic cleft represents a conserved site for protein–protein interactions, which could be relevant for miRNA-mediated gene silencing.

The GW182 RRM is dispensable for the interaction with AGO1 and miRNAs

To investigate the role of the RRM domain in GW182 function, we generated a protein mutant lacking the complete domain (GW182-ΔRRM) and tested its interaction with AGO1 and miRNAs. To this end, wild-type and mutant HA-epitope-tagged GW182 were transiently expressed in S2 cells and immunoprecipitated from cell lysates using anti-HA antibodies. We then tested for co-immunoprecipitation of endogenous AGO1 and miRNAs by western and northern blot, respectively.

We observed that GW182-ΔRRM interacted with endogenous AGO1 as efficiently as wild-type GW182 (Figure 4A, lanes 6 versus 5). Similarly, GW182-ΔRRM co-immunoprecipitated endogenous bantam (Figure 4A, lanes 6 versus 5). Together these results indicate that the RRM domain of GW182 is not required for the interaction with AGO1 and miRNAs.

GW182 RRM is dispensable for P-body localization

In previous studies, we showed that an N-terminal fragment of GW182 containing the N-terminal GW-repeats, the UBA domain and the Q-rich region, was necessary and sufficient to direct the protein to P-bodies (6). This protein fragment was also necessary and sufficient to promote the accumulation of AGO1 in P-bodies, a process that depends on GW182 (6). As expected from these previous studies (6), GW182-ΔRRM localized to cytoplasmic foci, which correspond to endogenous P-bodies as judged by the staining with anti-Trailer hitch (Tral) antibodies [Figure 4B and C; (3,25)]. GW182-ΔRRM also promoted the accumulation of AGO1 in P-bodies (Figure 4D–F), indicating that neither P-body localization nor the AGO1 interaction is impaired in this mutant, in agreement with the immunoprecipitation assays and with previous reports (6,8).

GW182 RRM contributes to target silencing by miRNAs

To investigate whether the RRM domain of GW182 plays a role in silencing, we established a complementation assay. In this assay, miRNA function is monitored using reporters in which the F-Luc Open reading frame (ORF)

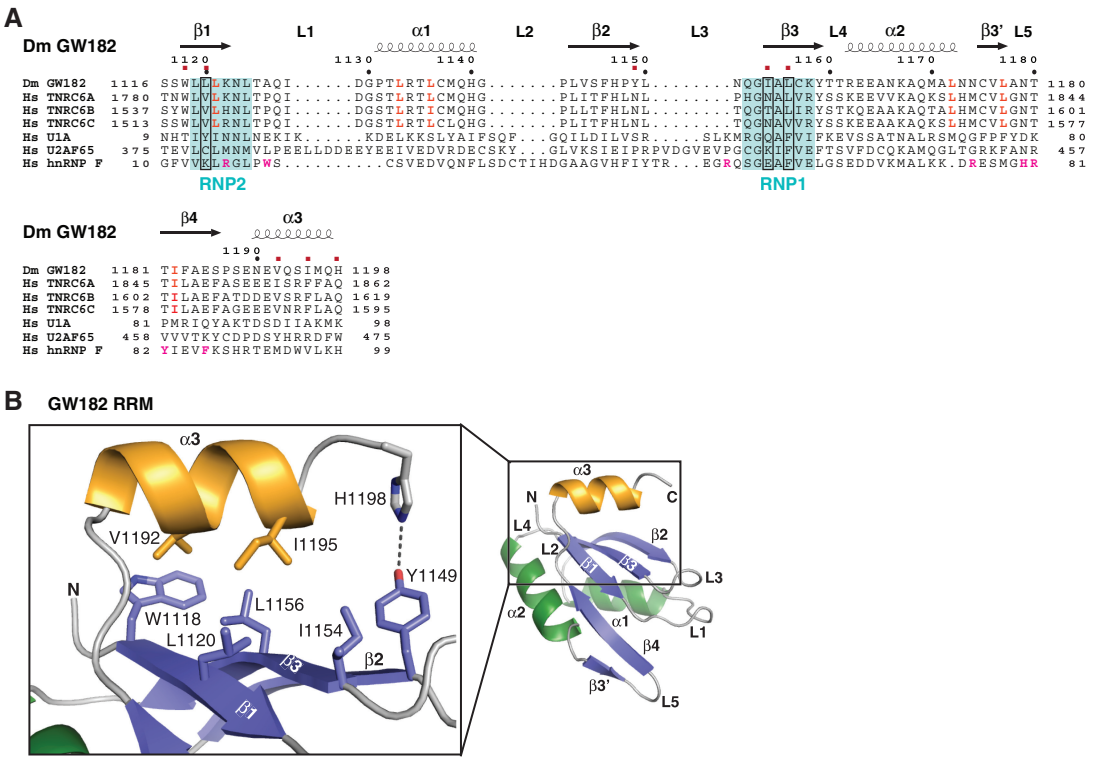

Figure 2. The C-terminal α-helix is a conserved feature of RRMs in GW182 proteins. (**A**) Structure-based alignment of RRM domains. The RNP1 and RNP2 motifs are shadowed in blue. Red dots above the sequences indicate residues mediating the interaction between the C-terminal helix α3 and the β-sheet of GW182 RRM. Red characters indicate residues lining the hydrophobic cleft on GW182 RRM and human TNRC6s. Magenta characters indicate residues affected by RNA binding in hnRNP F qRRM1. Dm, *Drosophila melanogaster;* Hs, *Homo sapiens*. Accession numbers are Dm GW182 (gi: 62473147); Hs TNRC6A (gi: 116805348), Hs TNRC6B (gi: 148491079), Hs TNRC6C (gi: 33413425), Hs U1A (gi: 4759156), Hs U2AF^{65} (gi: 6005926) and Hs hnRNP F (gi: 4826760). (**B**) Hydrophobic interactions between the C-terminal helix α3 and the β-sheet of GW182 RRM. Selected side chains are shown as sticks with oxygens in red. Hydrogen bonds are shown as dotted lines.

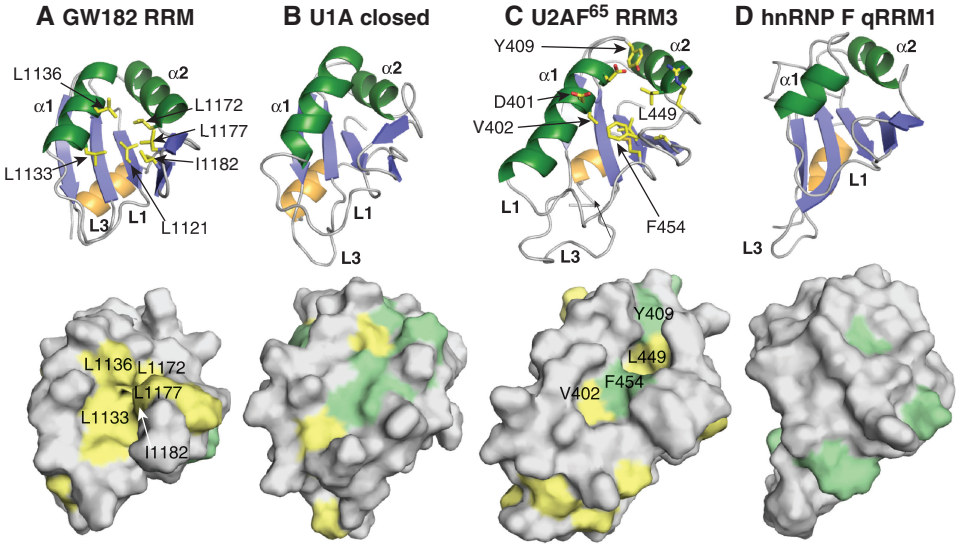

Figure 3. GW182 RRM exhibits a hydrophobic cleft on the helical face. (**A–D**) Top panels: ribbon representations of the RRMs from Figure 1 (same colors) with a view onto the helical face. Selected side chains are shown as sticks with carbons in yellow, oxygens in red and nitrogens in blue. Lower panels: corresponding surface representations with areas corresponding to aliphatic and aromatic residues in yellow and green, respectively.

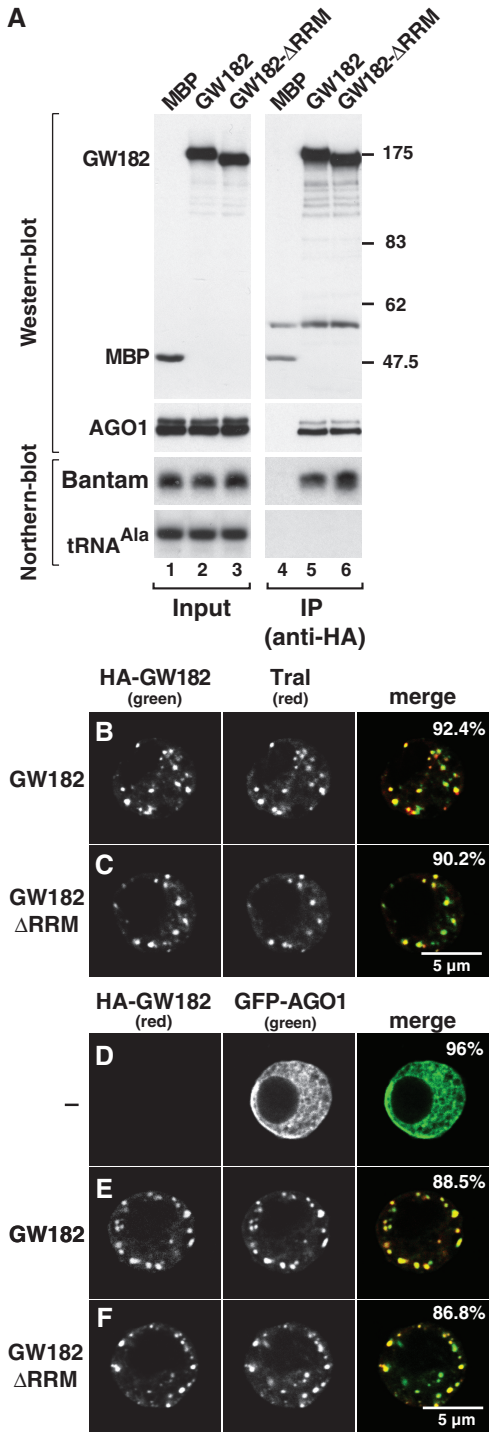

Figure 4. The GW182 RRM is dispensable for P-body localization and the interaction with AGO1 and miRNAs. (**A**) Lysates from S2 cells expressing λN-HA-tagged versions of MBP, wild-type GW182 or GW182-ΔRRM were immunoprecipitated using a monoclonal anti-HA antibody. Inputs (1.5%) and immunoprecipitates (30%) were analyzed by western blotting using a polyclonal anti-HA antibody. The association between GW182 and endogenous AGO1 or miRNAs was analyzed by western and northern blotting, respectively. $tRNA^{Ala}$ served as a loading control for the northern blots. (**B, C**) Confocal fluorescent micrographs of fixed S2 cells expressing HA-tagged fusions of full-length GW182 or GW182-ΔRRM. Cells were stained with affinity purified anti-Tral antibodies. The merged images show the HA signal in green and the anti-Tral signal in red. (**D–F**) GFP-tagged AGO1 was expressed in S2 cells. In (E, F), the effect of cotransfecting HA-GW182 or HA-GW182-ΔRRM on the localization of AGO1 was examined. The merged images show the GFP signal in green, the HA signal in red. The fraction of cells exhibiting a staining identical to that shown in the representative panel was determined by scoring at least 100 cells in two independent transfections performed per protein. Scale bar: 5 μm.

is cloned upstream of 3′-UTRs of *D. melanogaster* genes regulated by miRNAs. In particular, we used the previously characterized reporters F-Luc-CG10011 and F-Luc-CG3548 (silenced by miR-12) and F-Luc-Nerfin (silenced by miR-279 and miR-9b). We depleted endogenous GW182 using dsRNAs targeting the 5′- and 3′-UTR sequences of *GW182* mRNA.

miR-12 directs the F-Luc-CG10011 and F-Luc-CG3548 reporters to degradation, whereas miR-279 and miR-9b silence the F-Luc-Nerfin reporter mainly at the translational level (Figure 5A–D). Depleting endogenous GW182 suppressed silencing of these reporters and lead to a 3- to 8-fold increase of F-Luc activity [Figure 5E–H; (6–9)]. We then tested whether silencing could be restored by expressing either wild-type GW182 or the mutant lacking the RRM. These proteins were expressed from vectors including only the GW182 ORF, and thus were insensitive to the dsRNAs used to deplete the endogenous protein.

We found that in cells depleted of endogenous GW182, expressing wild-type GW182 restored silencing to levels comparable with those observed in control cells (Figure 5E–H). In contrast, the GW182 mutant lacking the RRM failed to efficiently restore silencing of either the F-Luc-CG10011 by miR-12, or of the F-Luc-Nerfin reporter by miR-279 (Figure 5E and G). The GW182-ΔRRM mutant fully restored silencing of the F-Luc-CG3548 reporter and of the F-Luc-Nerfin reporter when silencing was triggered by miR-9b (Figure 5F and H). The expression levels of wild-type and mutant GW182 proteins were comparable (Figure 4A). Together these results indicate that the RRM domain of GW182 is not essential, but contributes to silencing in a manner that is specific to miRNA-target pairs. This is so, independently of whether the target is silenced at the translational level or directed to degradation.

DISCUSSION

Proteins of the GW182 family are essential components of the miRNA pathway. They are required both to repress translation and to enhance degradation of miRNA targets (3,9). The insect and vertebrate members of this protein family are characterized by two domains predicted to be structured: a UBA and an RRM domain (1,2,4,6). Here, we show that the RRM domain of *D. melanogaster* GW182 adopts a classical RRM-fold, but lacks RNA-binding features. This domain is not essential for silencing, but rather contributes to silencing of a subset of miRNA-target pairs.

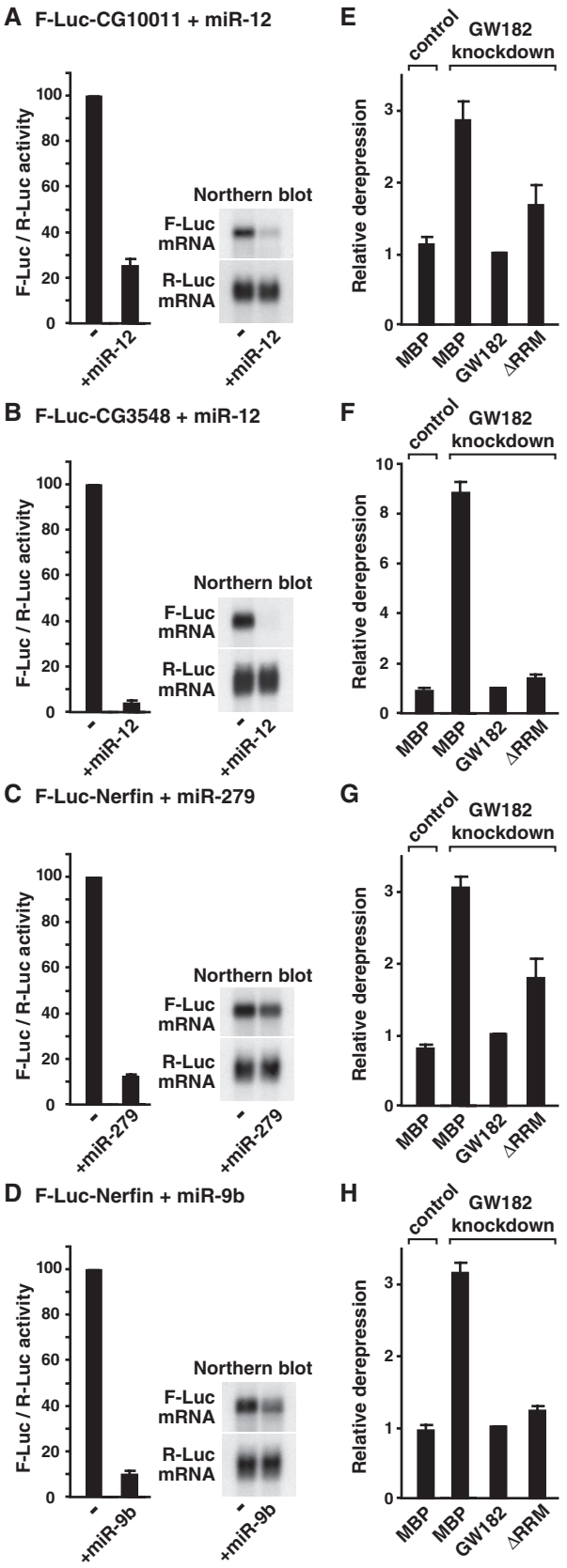

Figure 5. The GW182 RRM contributes to silencing. (**A–D**) S2 cells were transfected with a mixture of three plasmids: one expressing the indicated F-Luc reporters; another expressing miRNA primary transcripts (+miRNA) or the corresponding empty vector (−); and a third expressing *Renilla* luciferase (R-Luc). F-Luc activities were normalized to those of the *Renilla* luciferase transfection control and set to 100 in cells transfected with the empty vector (i.e. in the absence of the miRNAs). Mean values ± SD from three independent experiments are shown. Northern blot analysis of representative RNA samples are shown in the right panels. (**E–H**) S2 cells were treated with dsRNA targeting the 5′- and 3′-UTR of *GW182* mRNA. Control cells were treated with GFP dsRNA. These cells were subsequently transfected with a mixture of three plasmids as described in panels A–D. Plasmids encoding wild-type HA-GW182, HA-GW182-ΔRRM or HA-MBP were included in the transfection mixtures, as indicated. F-Luc activities were normalized to those of the *Renilla* luciferase transfection control as described in panel A. Graphs show relative fold derepression for each condition. Mean values ± SD from three independent experiments are shown.

The GW182 RRM lacks RNA-binding features

The RRM is an ancient protein domain of about 90 amino acids; it is present in all kingdoms of life and particularly prominent in eukaryotes. The core of the domain consists of one four-stranded anti-parallel β-sheet packed against two α-helices (26,27). Originally identified as an RNA-binding module, this domain can mediate protein–protein interactions in addition to, or instead of binding RNA [reviewed in (27)].

RRM–RNA interactions often involve two RNA bases stacking with the ring of conserved aromatic residues in the RNP motifs I and II; additional contacts may vary amongst different RRMs. In GW182 RRM, the conserved aromatic residues in the RNP1 and RNP2 motifs are substituted with aliphatic residues. This, together with the lack of detectable RNA-binding affinity, the absence of regions with positive electrostatic surface potential and the packing of the C-terminal α-helix against the β-sheet surface, suggest that GW182 RRM does not bind RNA.

A C-terminal α-helix masking the canonical RNA-binding surface was observed in other RRMs, including the N-terminal RRM of U1A (29), the CstF-64 RRM (37) and the qRRM1 of hnRNP F (31). Despite the α-helix, however, these domains do bind RNA.

In the U1A RRM, the C-terminal α-helix moves into an open conformation upon RNA binding (29), whereas in CstF-64 the α3 helix unfolds in the presence of RNA (37). In both cases, conserved aromatic residues in the RNP1 and RNP2 motifs become exposed and available for base-stacking interactions with RNA. The tight aliphatic interactions between helix α3 and the β-sheet surface of GW182 RRM makes it unlikely that this helix would swing away from the β-sheet as observed in U1A RRM. Finally, even if the C-terminal α-helix of GW182 would adopt an open conformation or unfold, the exposed β-sheet surface of GW182 lacks key aromatic and positively charged residues that could mediate RNA binding.

The C-terminal α-helix of the qRRM1 of hnRNP F does not change conformation in the presence of RNA (31). Nevertheless, as mentioned above, the qRRM1 of hnRNP F still binds RNA through aromatic and positively charged residues that are not on the β-sheet surface but are part of a short β-hairpin and loops L1 and L3 (31).

These residues are not present in GW182 RRM, indicating this domain is also unlikely to bind RNA in the quasi-canonical mode.

GW182 RRM: a protein interaction domain?

A survey of available structures of RRM domains in complex with other proteins revealed that RRM–protein interactions are very diverse, with no common features emerging [reviewed in (27)]. For instance, both Y14 and UPF3 RRMs interact with their binding partners (MAGOH and UPF2, respectively) through their β-sheet surfaces; however, the interaction interface between Y14 and MAGOH is mainly hydrophobic, whereas, the UPF3–UPF2 interaction is mediated by charged residues (35,36). Other RRMs use the helical surface for protein interactions. For instance, $U2AF^{65}$ RRM3 interacts with SF1 through residues located on helices α1 and α2 (30). In other cases, RRM–protein interactions are mediated by extensions or variations of secondary structural elements (27).

It is currently unclear how the GW182 RRM would interact with putative protein partners; but similar to $U2AF^{65}$ RRM3, the structure of the GW182 RRM reveals a hydrophobic cleft on the side of the β-sheet opposite to where helix α3 lies. This cleft is likely to engage in interactions with as yet unidentified partners.

Conservation of the GW182 RRM

The GW182 RRM is highly conserved (e.g. 58% identity between *D. melanogaster* GW182 and human TNRC6A), suggesting that in insect and vertebrate members of the GW182 protein family this domain adopts a similar fold with a similar function. In particular, the occlusion of the putative RNA-binding surface by the C-terminal α-helix and the presence of a hydrophobic cleft on the helical face are structural features conserved in RRM domains of GW182 proteins. Despite this conservation, the RRM is not essential for the silencing activity of GW182. Indeed, a GW182 protein lacking this domain can partially or fully rescue silencing in cells depleted of endogenous GW182. Nevertheless, it is still possible that this domain is important for silencing of only a specific subset of miRNA targets.

The conservation of the RRM domain in insects and vertebrates contrasts with the absence of this domain in the *C. elegans* proteins AIN-1 and AIN-2 (4,6). One possible explanation is that this domain plays a critical role in silencing a subset of miRNA targets only in insects and vertebrates. Alternatively, the *C. elegans* AIN-1 and AIN-2 may function in conjunction with additional partners that compensate for the lack of the RRM. Finally, the vertebrate and insect GW182 proteins may act in processes unrelated to silencing, which require the RRM domain. Indeed, inhibiting GW182 function by antibody injection in *D. melanogaster* syncytial stage embryos, leads to abnormal nuclear divisions, a phenotype that might or might not be a consequence of inhibiting the miRNA pathway (38).

Role of the GW182 RRM domain in silencing

In previous studies we showed that silencing by miRNAs is effected by AGO1-GW182 complexes (9). These complexes repress translation and/or enhance degradation of miRNA targets (3,9). GW182 RRM contributes to both of these mechanisms, as a GW182 protein that lacks the RRM is impaired in mediating both translational repression and mRNA decay. Although we cannot rule out that deleting the RRM domain affects GW182 folding, we consider this possibility unlikely because GW182-ΔRRM still interacts with AGO1 and miRNAs, localizes to P-bodies and silences a subset of miRNA targets. This raises the question: what step of silencing is affected by the deletion of the RRM domain? One possibility is that this domain contributes to target recognition by RISC, either by interacting with proteins bound to the mRNA target or by interfering with their binding, thereby increasing target accessibility. Alternatively, this domain may contribute to silencing downstream of target binding. For instance, the RRM may facilitate the interaction of RISC with either components of the translation machinery or general mRNA decay factors, and thus contribute to the effector step of silencing.

SUPPLEMENTARY DATA

Supplementary Data are available at NAR Online.

ACKNOWLEDGEMENTS

We are grateful to Christoph Fritzsch and Ajla Hrle for making some of the constructs used in this study, and to Sigrun Helms for excellent technical assistance.

FUNDING

Max Planck Society; Deutsche Forschungsgemeinschaft (DFG, FOR855 and the Gottfried Wilhelm Leibniz Program awarded to E.I.); Sixth Framework Programme of the European Commission through the SIROCCO Integrated Project LSHG-CT-2006-037900. Funding for open access charge: Max Planck Society.

Conflict of interest statement. None declared

REFERENCES

1. Eystathioy,T., Chan,E.K., Tenenbaum,S.A., Keene,J.D., Griffith,K. and Fritzler,M.J. (2002) A phosphorylated cytoplasmic autoantigen, GW182, associates with a unique population of human mRNAs within novel cytoplasmic speckles. *Mol. Biol. Cell*, **13**, 1338–1351.
2. Eystathioy,T., Jakymiw,A., Chan,E.K., Seraphin,B., Cougot,N. and Fritzler,M.J. (2003) The GW182 protein colocalizes with mRNA degradation associated proteins hDcp1 and hLSm4 in cytoplasmic GW-bodies. *RNA*, **9**, 1171–1173.
3. Eulalio,A., Behm-Ansmant,I. and Izaurralde,E. (2007) P bodies: at the crossroads of post-transcriptional pathways. *Nat. Rev. Mol. Cell Biol.*, **8**, 9–22.
4. Ding,L. and Han,M. (2007) GW182 family proteins are crucial for microRNA-mediated gene silencing. *Trends Cell Biol.*, **17**, 411–416.
5. Eulalio,A., Huntzinger,E. and Izaurralde,E. (2008) Getting to the root of miRNA-mediated gene silencing. *Cell*, **132**, 9–14.

6. Behm-Ansmant,I., Rehwinkel,J., Doerks,T., Stark,A., Bork,P. and Izaurralde,E. (2006) mRNA degradation by miRNAs and GW182 requires both CCR4:NOT deadenylase and DCP1:DCP2 decapping complexes. *Genes Dev.*, **20**, 1885–1898.
7. Rehwinkel,J., Behm-Ansmant,I., Gatfield,D. and Izaurralde,E. (2005) A crucial role for GW182 and the DCP1:DCP2 decapping complex in miRNA-mediated gene silencing. *RNA*, **11**, 1640–1647.
8. Behm-Ansmant,I., Rehwinkel,J. and Izaurralde,E. (2006) MicroRNAs silence gene expression by repressing protein expression and/or by promoting mRNA decay. *Cold Spring Harb. Symp. Quant. Biol.*, **71**, 523–530.
9. Eulalio,A., Huntzinger,E. and Izaurralde,E. (2008) GW182 interaction with Argonaute is essential for miRNA-mediated translational repression and mRNA decay. *Nat. Struct. Mol. Biol.*, **15**, 346–353.
10. Jakymiw,A., Lian,S., Eystathioy,T., Li,S., Satoh,M., Hamel,J.C., Fritzler,M.J. and Chan,E.K. (2005) Disruption of GW bodies impairs mammalian RNA interference. *Nat. Cell Biol.*, **7**, 1267–1274.
11. Liu,J., Rivas,F.V., Wohlschlegel,J., Yates., III,J.R., Parker,R. and Hannon,G.J. (2005) A role for the P-body component GW182 in microRNA function. *Nat. Cell Biol.*, **7**, 1261–1266.
12. Meister,G., Landthaler,M., Peters,L., Chen,P.Y., Urlaub,H., Luhrmann,R. and Tuschl,T. (2005) Identification of novel argonaute-associated proteins. *Curr. Biol.*, **15**, 2149–2155.
13. Landthaler,M., Gaidatzis,D., Rothballer,A., Chen,P.Y., Soll,S.J., Dinic,L., Ojo,T., Hafner,M., Zavolan,M. and Tuschl,T. (2008) Molecular characterization of human Argonaute-containing ribonucleoprotein complexes and their bound target mRNAs. *RNA*, **14**, 2580–2596.
14. Chu,C.Y. and Rana,T.M. (2006) Translation repression in human cells by microRNA-induced gene silencing requires RCK/p54. *PLoS Biol.*, **4**, e210.
15. Ding,L., Spencer,A., Morita,K. and Han,M. (2005) The developmental timing regulator AIN-1 interacts with miRISCs and may target the argonaute protein ALG-1 to cytoplasmic P bodies in *C. elegans*. *Mol. Cell*, **19**, 437–447.
16. Zhang,L., Ding,L., Cheung,T.H., Dong,M.-Q., Chen,J., Sewell,A.K., Liu,X., Yates,J.R. and Han,M. (2007) Systematic identification of *C. elegans* miRISC proteins, miRNAs, and mRNA targets by their interactions with GW182 proteins AIN-1 and AIN-2. *Mol. Cell*, **28**, 598–613.
17. Ding,X.C. and Großhans,H. (2009) Repression of C. elegans microRNA targets at the initiation level of translation requires GW182 proteins. *EMBO J.*, **28**, 213–222.
18. Till,S., Lejeune,E., Thermann,R., Bortfeld,M., Hothorn,M., Enderle,D., Heinrich,C., Hentze,M.W. and Ladurner,A.G. (2007) A conserved motif in Argonaute-interacting proteins mediates functional interactions through the Argonaute PIWI domain. *Nat. Struct. Mol. Biol.*, **14**, 897–903.
19. Diercks,T., Daniels,M. and Kaptein,R. (2005) Extended flip-back schemes for sensitivity enhancement in multidimensional HSQC-type out-and-back experiments. *J. Biomol. NMR*, **33**, 243–259.
20. Diercks,T., Coles,M. and Kessler,H. (1999) An efficient strategy for assignment of cross-peaks in 3D heteronuclear NOESY experiments. *J. Biomol. NMR*, **15**, 177–180.
21. Cornilescu,G., Delaglio,F. and Bax,A. (1999) Protein backbone angle restraints from searching a database for chemical shift and sequence homology. *J. Biomol. NMR*, **13**, 289–302.
22. Truffault,V., Coles,M., Diercks,T., Abelmann,K., Eberhardt,S., Luttgen,H., Bacher,A. and Kessler,H. (2001) The solution structure of the N-terminal domain of riboflavin synthase. *J. Mol. Biol.*, **309**, 949–960.
23. Coles,M., Hulko,M., Djuranovic,S., Truffault,V., Koretke,K., Martin,J. and Lupas,A.N. (2006) Common evolutionary origin of swapped-hairpin and double-psi beta barrels. *Structure*, **14**, 1489–1498.
24. Eulalio,A., Rehwinkel,J., Stricker,M., Huntzinger,E., Yang,S.F., Doerks,T., Dorner,S., Bork,P., Boutros,M. and Izaurralde,E. (2007) Target-specific requirements for enhancers of decapping in miRNA-mediated gene silencing. *Genes Dev.*, **21**, 2558–2570.
25. Eulalio,A., Behm-Ansmant,I., Schweizer,D. and Izaurralde,E. (2007) P-body formation is a consequence, not the cause of RNA-mediated gene silencing. *Mol. Cell Biol.*, **27**, 3970–3981.
26. Nagai,K., Oubridge,C., Jessen,T.H., Li,J. and Evans,P.R. (1990) Crystal structure of the RNA-binding domain of the U1 small nuclear ribonucleotide A. *Nature*, **348**, 515–520.
27. Maris,C., Dominguez,C. and Allain,F.H.-T. (2005) The RNA recognition motif, a plastic RNA-binding platform to regulate post-transcriptional gene expression. *FEBS J.*, **272**, 2118–2131.
28. Oubridge,C., Ito,N., Evans,P.R., Teo,C.H. and Nagai,K. (1994) Crystal structure at 1.92 A resolution of the RNA-binding domain of the U1A spliceosomal protein complexed with an RNA hairpin. *Nature*, **372**, 432–438.
29. Avis,J.M., Allain,F.H.-T., Howe,P.W.A., Varani,G., Nagai,K. and Neuhaus,D. (1996) Solution structure of the N-terminal RNP domain of U1A protein: the role of C-terminal residues in structure stability and RNA binding. *J. Mol. Biol.*, **257**, 398–411.
30. Selenko,P., Gregorovic,G., Sprangers,R., Stier,G., Rhani,Z., Kraemer,A. and Sattler,M. (2003) Structural basis for the molecular recognition between human splicing factors U2AF65 and SF1/mBBP. *Mol. Cell*, **11**, 965–976.
31. Dominguez,C. and Allain,F.H.-T. (2006) NMR structure of the three quasi RNA recognition motifs (qRRMs) of human hnRNP F and interaction studies with Bcl-x G-tract RNA: a novel mode of RNA recognition. *Nucleic Acids Res.*, **34**, 3634–3645.
32. Baker,N., Holst,M. and Wang,F. (2000) Adaptive multilevel finite element solution of the Poisson-Boltzmann equation; II: refinement at solvent accessible surfaces in biomolecular systems. *J. Comput. Chem.*, **21**, 1343–1352.
33. Laskowski,R.A., MacArthur,M.W., Moss,D.S. and Thornton,J.M. (1993) PROCHECK: a program to check the stereochemical quality of protein structures. *J. Appl. Crystallogr*, **26**, 283–291.
34. Shuker,S.B., Hajduk,P.J., Meadows,R.P. and Fesik,S.W. (1996) Discovering high affinity ligands for proteins: SAR by NMR. *Science*, **274**, 1531–1534.
35. Fribourg,S., Gatfield,D., Izaurralde,E. and Conti,E. (2003) A novel mode of RBD-protein recognition in the Y14-Mago complex. *Nat. Struct. Biol.*, **10**, 433–439.
36. Kadlec,J., Izaurralde,E. and Cusack,S. (2004) The structural basis for the interaction between nonsense-mediated mRNA decay factors UPF2 and UPF3. *Nat. Struct. Mol. Biol.*, **11**, 330–337.
37. Pérez Cañadillas,J.M. and Varani,G. (2003) Recognition of GU-rich polyadenylation regulatory elements by human CstF-64 protein. *EMBO J.*, **22**, 2821–2830.
38. Schneider,M.D., Najand,N., Chaker,S., Pare,J.M., Haskins,J., Hughes,S.C., Hobman,T.C., Locke,J. and Simmonds,A.J. (2006) Gawky is a component of cytoplasmic mRNA processing bodies required for early Drosophila development. *J. Cell Biol.*, **174**, 349–358.